J|A|C|S COMMUNICATIONS

Published on Web 03/31/2009

$CaFe_4As_3$: A Metallic Iron Arsenide with Anisotropic Magnetic and Charge-Transport Properties

Iliya Todorov,[†] Duck Young Chung,[†] Christos D. Malliakas,[‡] Quing'an Li,[†] Thomas Bakas,[§] Alexios Douvalis,[§] Giancarlo Trimarchi,[||] Kenneth Gray,[†] John F. Mitchell,[†] Arthur J. Freeman,[||] and Mercouri G. Kanatzidis*[,†]

Materials Science Division, Argonne National Laboratory, Argonne, Illinois 60439, Department of Chemistry, Northwestern University, Evanston, Illinois 60208, Department of Physics, University of Ioannina, Ioannina, Greece, and Department of Physics and Astronomy, Northwestern University, Evanston, Illinois 60208

Received January 23, 2009; E-mail: m-kanatzidis@northwestern.edu

The recent discovery of a new class of superconductors, $LaFeAsO_{1-x}F_x$, initiated extensive studies of the family of electron-correlated iron oxypnictide compounds *RE*OFeAs (*RE* = rare-earth element) with the ZrCuSiAs-type structure, whose superconducting transition temperatures T_c reach as high as 55 K for $SmFeAs(O_{1-x}F_x)$.[1−3] Later, it was found that superconductivity also exists in the series of compounds $AEFe_2As_2$ (*AE* = Ca, Sr, Ba) possessing the same FeAs layers but having the $ThCr_2Si_2$-type structure.[4] The superconductivity in this family can be induced either by partially substituting the cations with alkali metals (Na, K)[5−7] or by applying pressure.[8,9] So far, the record T_c in this system is 38 K, which was observed for $K_{0.4}Ba_{0.6}Fe_2As_2$.[5] The mechanism for superconductivity in these systems is not yet clear. In order to probe and fully understand the nature of the superconductivity, a materials database with a large number of related compounds is a prerequisite. In this context, we explored the system Ca/Fe/As and discovered the new metallic compound $CaFe_4As_3$, which exhibits an unusual tunnel framework structure, strong charge-transport anisotropy, and surprisingly complex magnetic properties as a function of temperature.

$CaFe_4As_3$ was synthesized as a single phase by heating a stoichiometric mixture of the elements in a Sn flux.[10] The needle-shaped black crystals of $CaFe_4As_3$ are stable in air and water. The thermal stability of $CaFe_4As_3$ was monitored by multiple heating/cooling cycles under vacuum using differential thermal analysis (DTA) and X-ray diffraction, and the resulting samples showed no phase transformation or decomposition up to 1150 °C.

$CaFe_4As_3$ crystallizes in the orthorhombic space group *Pnma* with an open 3D framework in which Fe and As form a covalent channel-like network and Ca^{2+} cations reside in the channels that run along the *b* axis of the orthorhombic cell (Figure 1). The covalent network is built of four crystallographically distinct Fe atoms and three As atoms. There are no bonding As−As distances in the structure. A closer look along the *ac* plane reveals that the network consists of Fe/As ribbons excised out of the PbO-type Fe_2As_2 layers of $CaFe_2As_2$ and arranged in a rectangular cross-pattern. The parallel Fe_2As_2 ribbons are aligned along the *b* axis and connected through Fe(4) to form the 3D network. The Fe_2As_2 layer is a building unit in the structures of binary FeAs as well as the recently discovered superconducting layered materials.

The Fe−As distances in $CaFe_4As_3$ fall into two different groups depending on the coordination environment of the Fe atoms. The short Fe−As distances, 2.380(2)−2.465(1) Å, are found around Fe(1), Fe(2), and Fe(3), which are tetrahedrally coordinated by

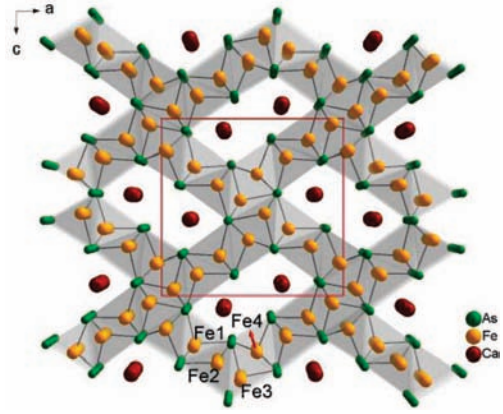

Figure 1. Projection view along the *b* axis of $CaFe_4As_3$.

As(1), As(2), and As(3), (293 K structure; see Table S4 in the Supporting Information). These distances are similar to those observed in $CaFe_2As_2$ and $K_{0.4}Ba_{0.6}Fe_2As_2$.[5,6] The As−Fe−As angles for Fe(1), Fe(2), and Fe(3), which range from 93.63(5) to 116.39(4)°, strongly deviate from the angle of ideal tetrahedral geometry (Table S4). The second group of Fe−As distances, around Fe(4), are longer [in the range 2.427(1)−2.610(1) Å] because of its higher coordination number and square-pyramidal geometry. The As−Fe−As angle in this geometry varies between 85.18(2)° and 104.67(4)°. Each Ca^{2+} ion sits at the center of a monocapped trigonal prismatic coordination by two As(1), two As(2), two As(3), and an additional capped As(3) atom.

Formal charges can be assigned according to the octet rule by assuming complete electron transfer from the cations to the anions. The formula of $CaFe_4As_3$ can be rationalized as $(Ca^{2+})[(Fe^{2+})_3(Fe^{+})(As^{3-})_3]$. This counting is in agreement with the Mössbauer measurements, which revealed that the compound has three formally Fe^{2+} tetrahedrally coordinated ions and one formally Fe^{1+} five-coordinate ion.

Electrical resistivity measurements performed on a single crystal of $CaFe_4As_3$ showed typical metallic behavior over the temperature range 5−300 K with significant anisotropy. The electrical resistivity measured parallel to the *b* axis (the needle crystal direction) is 6 times lower than that measured perpendicular to the *b* axis (Figure 2a). In addition, the latter shows a peak with an anomaly at ∼25 K, which is consistent with the temperature at which a magnetic transition occurs (see below).

The Mössbauer spectrum confirms the presence of Fe^{2+} and Fe^{1+} centers in the compound. The spectrum of $CaFe_4As_3$ measured at room temperature[11] shows only paramagnetic quadrupole-splitting

[†] Argonne National Laboratory.
[‡] Department of Chemistry, Northwestern University.
[§] University of Ioannina.
[||] Department of Physics and Astronomy, Northwestern University.

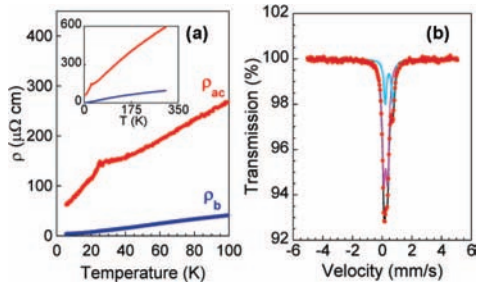

Figure 2. (a) Typical electrical resistivity from a single-crystal sample measured perpendicular (red) and parallel (black) to the *b* axis of $CaFe_4As_3$ from 5 to 100 K. The inset represents the resistivity data up to room temperature. (b) Mössbauer spectrum of $CaFe_4As_3$ recorded at room temperature (fitted with two doublets, as described in the text).

contributions, which have the characteristics of two different doublets (Figure 2b). The resulting Mössbauer parameters of the two components (1 and 2) used to fit this spectrum are $\delta_1 = 0.35(1)$ mm s^{-1}, $QS_1 = 0.25(1)$ mm s^{-1}, $A_1 = 74(2)\%$, $\Gamma_1 = 0.26(1)$ mm s^{-1} and $\delta_2 = 0.57(1)$ mm s^{-1}, $QS_2 = 0.52(1)$ mm s^{-1}, $A_2 = 26(2)\%$, $\Gamma_2 = 0.23(1)$ mm s^{-1}, where δ, QS ($=e^2qQ/2$), A, and Γ correspond to the isomer shift (relative to α-Fe), quadrupole splitting, relative absorption area, and full line width at half-maximum, respectively. The ratio of the absorption areas of the two components, A_2/A_1, has a value of $^{26}/_{74} \approx {}^{1}/_{3}$. With the assumption that the four nonequivalent crystallographic sites of $CaFe_4As_3$ accommodating Fe ions have equal Debye−Waller factors, which is applicable for crystalline solids,[12] this ratio corresponds to the ratio of the populations of the formally Fe^{1+} and Fe^{2+} ions in the structure of $(Ca^{2+})[(Fe^{2+})_3(Fe^{+})(As^{3-})_3]$. In addition, the isomer shift value of the component with the majority absorption area is in the range of isomer shift values recorded for As-coordinated formally Fe^{2+} ions in $BaFe_2As_2$.[4] On the other hand, the fact that $QS_1 < QS_2$ indicates a larger distortion of the surrounding As^{3-} ion environment for the iron ions corresponding to component 2 than for those of component 1. Taking all these results into account, we can suggest that the major component 1 corresponds to the three formally Fe^{2+} tetrahedrally coordinated ions and the minor component 2 to the one formally Fe^{1+} five-coordinate ion in the $CaFe_4As_3$ structure.

Magnetization measurements on polycrystalline samples of $CaFe_4As_3$ were performed in the zero-field-cooling (ZFC) and field-cooling (FC) modes using applied fields of 100 and 1000 Oe.[13] The initial ZFC measurement was done using an applied field of 100 Oe and followed by the FC measurement at the same field, while the measurements at an applied field of 1000 Oe were done successively after the sample was heated to 300 K and cooled to 5 K in zero field. The compound does not follow Curie−Weiss behavior. When a 100 Oe field was applied with ZFC, a steep transition at ∼40 K and a broad maximum at ∼84 K were observed in the magnetic moment (Figure 3a). When the applied field was increased to 1000 Oe, both the ZFC and FC curves showed a broad maximum at ∼92 K, indicative of the characteristic antiferromagnetic transition at this temperature. The peak of the 1000 Oe ZFC curve at lower temperatures broadened further in comparison with that at 100 Oe, and its maximum also shifted to lower temperature (∼25 K). Hysteresis between the ZFC and FC curves starting just below 300 K and widening at ∼90 K was observed at applied fields of 100 and 1000 Oe.

Anisotropic magnetization measurements on a single crystal oriented parallel and perpendicular to the needle direction (i.e., along the *b* axis and in the *ac* plane in the crystal structure, respectively) at a magnetic field of 2000 Oe were performed (Figure 3b). When the magnetic field was applied along the needle direction, the ZFC

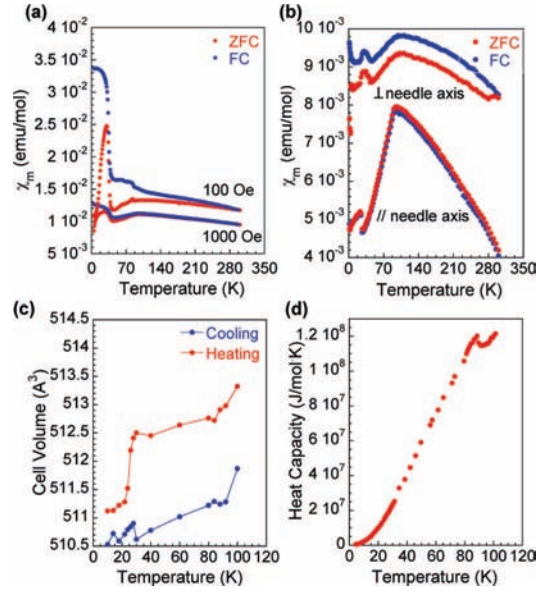

Figure 3. (a) Molar magnetic susceptibility of a powder sample of $CaFe_4As_3$ from magnetization vs temperature measurements of $CaFe_4As_3$ recorded between 5 and 300 K at applied magnetic fields of 100 and 1000 Oe in the ZFC and FC modes. (b) Anisotropic molar magnetic susceptibility measured on a single-crystal sample of $CaFe_4As_3$ at 2000 Oe. (c) Unit cell volume of $CaFe_4As_3$ as a function of temperature measured upon heating and cooling from 10 to 100 K. (d) Molar heat capacity measured from 10 to 110 K with no applied field.

and FC measurements showed two magnetic maxima at ∼23 and ∼96 K. As for the ZFC and FC measurements on the polycrystalline sample, there was a steep increase and decrease in the magnetic moment values. The lack of hysteresis suggests that no magnetic interactions between the Fe spins exist along this direction. This is attributed to the fact that the Fe atoms are far apart [Fe−Fe distances of 3.7403(3) Å]. In contrast, when the field was applied perpendicular to the needle direction (in the *ac* plane), where the Fe−Fe distances are 2.593(1) and 2.851(1) Å, the ZFC and FC measurements showed that the two magnetic transitions broaden and shift somewhat to higher temperatures. The magnetic transition at ∼96 K appears to be antiferromagnetic in nature, while the one at ∼23 K is ferromagnetic (i.e., the magnetization in ZFC mode is lower than that in FC mode below ∼23 K and decreases with decreasing temperature). There is also a hysteresis between the ZFC and FC curves up to room temperature. Apparently, there are strong magnetic interactions between the Fe spins in the *ac* plane, where the Fe−Fe distances are short. This magnetic anisotropy is consistent with the transition observed only in the *ac*-plane electrical resistivity plot at ∼23 K (Figure 2a, red curve). In addition, the unit cell volume shows abnormal changes as a function of temperature, with transitions observed at ∼23 and ∼90 K (Figure 3c). It is evident that the observed magnetic transitions are accompanied by subtle structural distortions. Specifically, at these temperatures, the small but sudden changes in the interatomic distances between the Fe atoms in the *ac* plane appear to have a profound effect on the magnetic exchange interactions.

Temperature-dependent specific heat measurements[14] were also performed on single crystals of $CaFe_4As_3$ and confirmed the transition at ∼90 K (Figure 3d). Interestingly, no apparent anomaly in the specific heat was observed near the first transition point (∼25 K), even with the application of magnetic fields (1000 and 5000 Oe). This suggests that the two transitions have a different origin. A Debye temperature (Θ_D) of 210(3) K and an electronic specific heat coefficient (γ) of 204(15) mJ mol^{-1} K^{-2} were calculated from

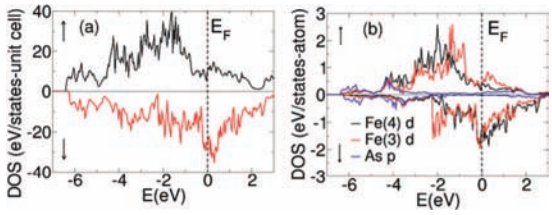

Figure 4. (a) (top) Total DOS of $CaFe_4As_3$ in the ferromagnetic configuration and (bottom) DOS projected onto the Fe(3) and Fe(4) d orbitals. (b) DOS for the p orbital of one of the As atoms shared between Fe(3) and Fe(4). Both spin-up and spin-down DOS are plotted.

the low-temperature region of the data (4−48 K) by fitting the Debye function. The relatively large γ value suggests a moderate heavy-fermion behavior. At this stage, the origin of the two transitions and their relationship to the moderate heavy-fermion behavior is unknown. Neutron diffraction experiments could answer these questions.

Since Mössbauer spectroscopy and the magnetization measurements cannot resolve the direction and magnitude of the magnetic moments at the Fe sites of $CaFe_4As_3$, density functional theory calculations can be very useful in providing insight into such details of the magnetic structure. We used the all-electron full-potential linearized augmented plane-wave method[15] with the generalized gradient approximation[16] to the exchange and correlation functional. The lattice vectors and atomic positions were kept fixed at their experimental values measured at 15 K. Starting the self-consistent calculation by setting the starting moments on the Fe sites parallel and with a magnitude of $1.1\mu_B$, we found a stable ferromagnetic configuration 0.656 eV/formula unit lower in energy than the nonmagnetic solution. In this ferromagnetic structure, the tetrahedrally coordinated Fe(1), Fe(2), and Fe(3) sites show moments of 1.70, 1.84, and $1.00\mu_B$, respectively, while the five-coordinate Fe(4) site shows a moment of $2.06\mu_B$. Finding this stable ferromagnetic configuration is consistent with the interpretation that the observed peak in the magnetic susceptibility at 25 K (see Figure 3a,b) indeed corresponds to a ferromagnetic transition. The site-dependence of the Fe magnetic moment suggests that this quantity is sensitive to the Fe−As and Fe−Fe bond lengths and Fe−As−Fe angles of the Fe_2As_2 ribbons.

Indeed, a recent theoretical analysis of the magnetic structure of the related layered iron pnictides[17] showed that the Fe moment is very sensitive to the p−d hybridization and tends to decrease with decreasing Fe−As distance.[18] Such a trend is observed in $CaFe_4As_3$, in which the largest magnetic moment, $2.06\mu_B$, is found at the five-coordinate Fe(4) site, where the Fe−As distances vary between 2.43 and 2.61 Å, while the lowest magnetic moment is found for Fe(3), where the average Fe−As bonding distance is 2.40 Å. Figure 4a shows the total density of states (DOS) of this ferromagnetic configuration. Here, the large DOS at the Fermi energy (E_F) confirms the metallic character of this material. The local DOS projected onto the Fe(3) and Fe(4) d orbitals (lower panel) shows that the imbalance between the spin-up and spin-down local DOS is larger on the Fe(4) site than on the Fe(3) site, and this is reflected by the larger magnetic moment on Fe(4). The As p states lie mostly between −4.5 and −3.5 eV (Figure 4b) and hybridize with the Fe d orbitals in this energy interval.

In conclusion, the novel network of $CaFe_4As_3$ implies that the Fe_2As_2 layers are amenable to rearrangements that can lead to new iron arsenides. The Mössbauer, magnetic, and electrical resistivity data for $CaFe_4As_3$ reveal complex magnetic behavior and possible instabilities. The physical properties of $CaFe_4As_3$ require further studies, including temperature-dependent neutron diffraction experiments and studies of magnetization under pressure.

Acknowledgment. This project was supported by the U.S. Department of Energy, Office of Basic Energy Sciences, under Contract DE-AC02-06CH11357. We thank Dr. M. Pissas, NRCPS "Demokritos", Athens, for the magnetic susceptibility measurements on the polycrystalline sample.

Supporting Information Available: X-ray crystallographic data (CIF), tables of data collection parameters, details of the structure solution, refinement results, atomic positions, displacement parameters, anisotropic displacement parameters, and specific heat data from 4 to 48 K fitted with the Debye formula. This material is available free of charge via the Internet at http://pubs.acs.org.

References

(1) Kamihara, Y.; Watanabe, T.; Hirano, M.; Hosono, H. *J. Am. Chem. Soc.* **2008**, *130*, 3296.
(2) Takahashi, H.; Igawa, K.; Arii, K.; Kamihara, Y.; Hirano, M.; Hosono, H. *Nature* **2008**, *453*, 376.
(3) Ren, Z.-A.; Che, G.-C.; Dong, X.-L.; Yang, J.; Lu, W.; Yi, W.; Shen, X.-L.; Li, Z.-C.; Sun, L.-L.; Zhou, F.; Zhao, X.-Z. *Europhys. Lett.* **2008**, *83*, 17002.
(4) Rotter, M.; Tegel, M.; Johrendt, D.; Schellenberg, I.; Hermes, W.; Pottgen, R. *Phys. Rev. B* **2008**, *78*, 020503(R) .
(5) (a) Rotter, M.; Tegel, M.; Johrendt, D. *Phys. Rev. Lett.* **2008**, *101*, 107006. (b) Christianson, A. D.; Goremychkin, E. A.; Osborn, R.; Rosenkranz, S.; Lumsden, M. D.; Malliakas, C. D.; Todorov, I. S; Claus, H.; Chung, D. Y.; Kanatzidis, M. G.; Bewley, R. I.; Guidi, T. *Nature* **2008**, *456*, 930.
(6) Sasmal, K.; Bing, L.; Lorenz, B.; Guloy, A.; Chen, F.; Xue, Y.-Y.; Chu, C.-W. *Phys. Rev. Lett.* **2008**, *101*, 107007.
(7) Gooch, M.; Lv, B.; Lorenz, B.; Guloy, A. M.; Chu, C.-W. *Phys. Rev. B* **2008**, *78*, 180508(R).
(8) Park, T.; Park, E.; Lee, H.; Klimczuk, T.; Bauer, E. D.; Ronning, F.; Thompson, J. D. *J. Phys. Condens. Matter* **2008**, *20*, 322204.
(9) Torikachvili, M. S.; Bud'Ko, S. L.; Ni, N.; Canfield, P. C. 2008, arXiv: 0810.0241v1. arXiv.org e-Print archive. http://arxiv.org/abs/0810.0241v1 (accessed March 17, 2009).
(10) Starting materials for the preparation of $CaFe_4As_3$ were Ca (Alfa Aesar, granules, 99.5%), Fe (Cerac, powder, 99.9%), As (Alfa Aesar, powder, 99.99%), and Sn (Cerac, shot, 99.9%). All of the manipulations were done in a nitrogen-filled glove box with moisture and oxygen levels less than 1 ppm. Ca (0.0407 g, 1 mmol), Fe (0.223 g, 4 mmol), As (0.225 g, 3 mmol), and 5 g of Sn pieces were added to an alumina crucible, which was placed in a quartz ampoule and subsequently sealed under a reduced pressure of 10^{-4} Torr. This assembly was heated to 650 °C for 12 h, held there for a period of 6 h, then heated to 1123 K for 12 h, held for 6 h, and slowly cooled to 873 K for 12 h. At this temperature, the liquid Sn flux was filtered by centrifugation. The resulting product was metallic needlelike crystals.
(11) Mössbauer measurements were carried out with a constant-acceleration spectrometer equipped with a $^{57}Co(Rh)$ source calibrated with α-Fe, relative to which isomer shift values are reported.
(12) Gibb, T. C.; Greenwood, N. N. *Mossbauer Spectroscopy*; Chapman and Hall: London, 1971.
(13) Magnetization measurements were carried out using a SQUID magnetometer (Quantum Design MPMS-XL) over the temperature range 5−300 K. Anisotropic magnetization measurements on $CaFe_4As_3$ single crystals were performed using a Quantum Design MPMS SQUID magnetometer. Temperature-dependent data were collected in both the ZFC and FC modes between 2 and 300 K, with an applied field of 2000 Oe. Field-dependent magnetic measurements were acquired at 5, 32, and 105 K with the field swept from−50 to 50 kG. No background correction for the sample holder (straw and kapton tape) was performed. Space group, *Pnma*; a = 11.8953(12) Å, b = 3.7430(3) Å, c = 11.6100(10); V = 516.92(8) Å^3; d_{calcd} = 6.274 g/cm^3; R1 = 0.0308, wR2 = 0.0628 (see the Supporting Information for details).
(14) (a) Specific heat capacity measurements on $CaFe_4As_3$ were performed with a Quantum Design PPMS commercial instrument over the temperature range 4.6−100 K in zero field by a relaxation method using the "Two-Tau Model" (ref 14b). Single crystals were mounted on the sample puck using special low-temperature grease (Quantum Design). Specific heat data were corrected for background (stage and grease). (b) Hwang, J. H.; Lin, K.; Tien, C. *Rev. Sci. Instrum.* **1997**, *68*, 94.
(15) Wimmer, E.; Krakauer, H.; Freeman, A. J. *Phys. Rev. B* **1981**, *24*, 864.
(16) Perdew, J. P.; Burke, K.; Ernzerhof, M. *Phys. Rev. Lett.* **1996**, *77*, 3865.
(17) Wu, J.; Phillips, P.; Castro-Neto, A. H. *Phys. Rev. Lett.* **2008**, *101*, 126401.
(18) Mirbt, S.; Sanyal, B.; Isheden, C.; Johansson, B. *Phys. Rev. B* **2003**, *67*, 155421.

JA900534H